V

Publication V

J. Oksanen and J. Tulkki, *Fast all-optical flip-flop memory exploiting the electric field nonlinearity of coherent laser amplifiers*, IEEE Journal of Quantum Electronics **42**, pp. 509-516 (2006).

Fast All-Optical Flip-Flop Memory Exploiting the Electric Field Nonlinearity of Coherent Laser Amplifiers

Jani Oksanen and Jukka Tulkki

***Abstract*—The coherent nonlinear feedback in an integrated optical flip-flop is studied in order to demonstrate device applications of laser amplifiers operated above the laser threshold. The nonlinear feedback is provided by the stabilizing fields of the laser amplifiers, interfering with coherent optical reference fields. In both stable states of the flip-flop, the nonlinear feedback allows the laser amplifiers to maintain an ever present photon population in the laser modes and to have an approximately constant carrier population. This enables faster response (switching times below 25 ps are reached in this work) than in conventional active optical flip-flop structures. The operation of the flip-flop is studied using a rate equation model accounting for the carrier densities and the complex electric fields in the different cavity modes of the laser amplifiers.**

***Index Terms*—Laser amplifiers, optical bistability, optical memory.**

I. Introduction

IN ELECTRONICS, a bit of information can be stored by at least two commonly known purely electronic (in distinction to magnetic) methods. For one, it is possible to use capacitors, which can store charge and thus remember their state for some period of time (the time depending mostly on the external control circuitry). Another, more complex method, is based on the bistability created by nonlinear feedback.

In the optical domain optical resonator structures can store light for short periods of time, like capacitors in electronic domain. However, due to the extremely short photon lifetimes and the lack of control methods, they are not suitable for memory operation. On the other hand, bistable systems of lasers have been shown to be capable of storing information and different configurations of memory units have been proposed [1]–[9]. In most of these systems the lasers are operated on both sides of the laser threshold and the operating speed is often limited by the need to create the photon field from the spontaneously emitted photons. Furthermore, the carrier density in the lasers needs to change significantly to switch state.

This work presents an alternative way of realizing the nonlinear feedback needed for bistable operation of a two-laser system. The method makes it possible to stay above the lasing threshold in both the lasers and thus to minimize the changes in the carrier densities. This will enhance the modulation properties of the device. Section II describes the operation principle of the flip-flop qualitatively, while Section III introduces a mathematical rate equation model for quantitative treatment. In Section IV, the rate equation model is used to simulate the operation of the flip-flop. In the appendix, the analytic results presented in Section III are derived in detail from the simplified steady-state model.

Manuscript received December 16, 2005; revised January 31, 2006.

The authors are with the Laboratory of Computational Engineering, Department of Electrical and Communications Engineering, Helsinki University of Technology, Espoo FIN-02015 HUT, Finland (e-mail: jani.oksanen@lce.hut.fi; jukka.tulkki@hut.fi).

Digital Object Identifier 10.1109/JQE.2006.874004

II. Introduction of the Structure and Operation

A. Flip-Flop Structure

The general description of the coherent optical flip-flop (COFF) is best formulated by using a simplified model composed of two gain clamped semiconductor optical amplifiers (laser amplifiers), bandstop filters, external signal sources and two optical isolators [Fig. 1(a)]. The optical isolators of the simplified model are replaced by active antireflectors in the more complete structure, shown in Fig. 1(b).

The two current driven laser amplifiers [marked as L_1 and L_2 in Fig. 1(a) and (b)] play the key role in the operation. They share three optical modes, denoted by wavelengths λ_1, λ_2, and λ_3. In laser L_1 the lasing occurs at λ_1 and in laser L_2 at λ_2. Modes that are not lasing (λ_2 and λ_3 in L_1 and λ_1 and λ_3 in L_2) have larger losses. Therefore, there is optical power in these modes only if it is injected by an external field. Both laser modes are phase locked to external master lasers (also at wavelengths λ_1 and λ_2), so that all the fields can be considered coherent and to have a well defined phase.

The lasers are coupled to each other so that wavelength λ_1 from laser L_1 is guided to L_2, and wavelength λ_2 is guided from L_2 to L_1. This far the situation is very similar to the previously introduced bistable coupled laser system, except for a somewhat more complicated structure [2]. The drastic modification to the previous designs is adding the coherent bias fields E_{B1} and E_{B2} to the inputs of L_1 and L_2.

B. Operation of the Unbiased Flip-Flop

With the bias signals E_{B1} and E_{B2} set to zero, the COFF operates like the unbiased flip-flop introduced in [2]. The operation principle of the unbiased flip-flop has much in common with the COFF, and its operation is, therefore, briefly introduced as well.

After switching on the unbiased flip-flop, it drifts to a state where one laser (say L_1) is switched on, and the output of L_1 at λ_1 injected to L_2 quenches lasing in L_2. The output port gives out no radiation in this state but the inverted output port does (see Fig. 1 for the port definitions). Switching the flip-flop to

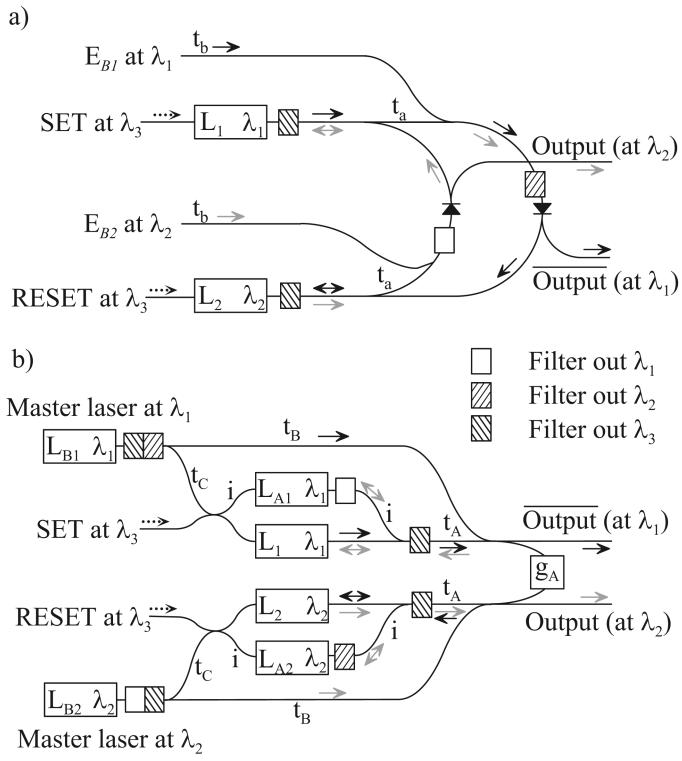

Fig. 1. Schematic representation of the structure. (a) Idealized model with the two lasers L_1 and L_2 acting as the core of the flip-flop. (b) Complete device structure including all the necessary components, i.e., six lasers connected by waveguides having electric field transmission coefficients $t_k, k \in \{a, b, A, B, C\}$, an (optional) amplifier with gain g_A and filters to remove unwanted frequencies. Injecting light in the SET and RESET ports sets and resets the flip-flop, respectively. The output and the inverted output (denoted by the overhead bar) can be read from the corresponding output ports at λ_2 and λ_1, respectively. Both the models are functionally equivalent: the optical isolators of (a) are just replaced by the more complex antireflector structures in (b), where the bias signals E_{B1} and E_{B2} are also obtained directly from lasers L_{B1} and L_{B2}. The arrows in the figure denote the principal propagation directions of the modes λ_1 (black), λ_2 (light gray), and λ_3 (dotted black).

the state where the output (at λ_2) is high is done by injecting an external signal at λ_3 to L_1 (SET-state, SET-operation). The external signal is amplified and robs power from the laser mode λ_1. With sufficiently strong external injection, lasing starts in L_2 at λ_2, because the optical injection at λ_1 to L_2 is reduced. The setting on of the laser field in L_2 is seeded by the spontaneously emitted photons. Consequently, there is a delay before the power in the laser mode starts to rise, and strong relaxation oscillations may accompany the setting on of the laser. Even after the external injection to L_1 is removed, L_2 remains lasing and quenches lasing in L_1. Due to the symmetry of the structure injecting a signal at λ_3 to L_2, makes L_1 active and disables lasing in L_2 (RESET-operation). A SET (RESET) -operation has no net effect on the state of the system, if the system is initially in the SET (RESET) state.

Note that another type of a flip-flop structure with potentially fast operation based on Mach–Zehnder interferometers and semiconductor optical amplifiers has also been reported [10]. Like most flip-flop structures, this device also relies on nonlinear feedback. However, the nonlinearity is produced by varying the phase shifts in the interferometer arms, not the optical power, as in this work.

C. Operation Principle of the COFF

The limitation in the unbiased flip-flop is that one laser is always operating below the laser threshold, and it takes a relatively long time to switch it back on. The coherent biasing offers a way to circumvent this additional switch-on delay by providing a nonlinear feedback mechanism that allows the lasers to stay above the threshold in both stable states.

The nonlinear feedback in the flip-flop is based on the interference of coherent fields and on the inherent properties of laser amplifiers, rather than on operating a laser amplifier on both sides of the laser threshold. The output power of the laser mode of a laser amplifier decreases linearly as a function of the input power at the signal frequency. Here however, the output of the laser, say L_2 at λ_2, is injected to L_1 only after it has interfered with the bias signal E_{B2}. The output power of L_1 then is not linear with respect to the output power P_2 of L_2, but of the form $P_0 - (E_{B2} + \sqrt{P_2})^2$, where P_0 is the maximum output power of L_1 and the values are scaled to show the general form of the nonlinearity in the simplest form.

The nonlinear feedback in the COFF can be adjusted so that there are two stable states that are suitable for flip-flop operation. In these states laser L_1 (or L_2 in the other state) has approximately all of its optical power in the laser mode while the electric field of the laser mode in L_2 (L_1) is approximately equal to $-E_{B2}(-E_{B1})$. The feedback to L_1 (L_2) is then approximately zero. These approximative states result directly from the nonlinear feedback between the lasers. The feedback will be studied in greater detail later.

The advantages of the COFF are all based on there being an approximately constant carrier density in each laser at all times (except during switching the state) and on the power of the laser mode never needing to build up from zero when the system changes state. The first fact also implies that there is practically no net transfer of carriers between the lasers during switching. The relatively large optical power present in the cavity also reduces the total carrier lifetime in the cavity and makes it possible to make the conventional relaxation oscillations disappear, like in quantum-cascade lasers [11].

D. Complete Model

The complete COFF model [Fig. 1(b)] used in numerical simulations is identical in the basic operation principles to the idealized model described above and in Fig. 1(a). However, the model now includes the master lasers providing the bias signals E_{B1} and E_{B2} and the reference phases (lasers L_{B1} and L_{B2}). It also uses interferometric antireflectors to replace the optical isolators, used for simplicity in Fig. 1(a). The antireflectors are formed by lasers L_{A1} and L_{A2} and the interferometric waveguide junctions. They are not functionally completely equivalent to optical isolators, but they are adequate for preventing backward propagation of the unwanted signals in this system. In addition they are suitable for integration, whereas integration of optical isolators is not feasible with current technology. An (optional) amplifier denoted as g_A may also be used to compensate for the losses in the waveguide junctions.

III. Theory of Operation

The quantitative description of COFF is started by introducing the rate equations using vector representations for the carrier densities and electric fields in the lasers. The use of electric fields instead of the conventional photon densities is necessary to account for the phase dependence of the interference. This gives the equations a highly nonlinear nature. The equations are very similar in appearance to the rate equations describing a single phase locked laser from which the equations are derived [12]. In Section III-B the theoretical model is completed by introducing the matrix and vector parameters that are needed to represent the two structures of Fig. 1.

The stable states of the system, analytically derived from a simple steady-state model in the Appendix, are presented in Section III-C. In Section III-D, the steady-state equations are used to investigate the phase shifts involved in the phase locking of the lasers to minimize the effects of chirping.

A. Rate Equations

Rate equations are a convenient way to model a system of phase-locked lasers with several cavity modes and coupled by a waveguide network. In vector form the equations can be written as

$$\frac{d\mathbf{n}}{dt} = \frac{I}{qV} - \sum_{j\in\{U,B,C\}} 2\xi v \mathbf{G}_j(\mathbf{n})|\mathbf{E}_j|^2 - \frac{\mathbf{n}}{\tau} \tag{1}$$

$$\frac{d\mathbf{E}_j}{dt} = \frac{v}{2}[\mathbf{G}_j(\mathbf{n}) - \boldsymbol{\alpha}_j + i\Delta\boldsymbol{\omega}_j(\mathbf{n})]\mathbf{E}_j + \frac{v}{2L}\mathbf{E}_j^{\text{ext}} + \frac{v}{2L}\mathbf{M}_j\mathbf{E}_j. \tag{2}$$

Each component of the carrier density $\mathbf{n}$ and of the propagating complex electric field $\mathbf{E}_j$ of the cavity mode $j \in \{U, B, C\}$ (U stands for the mode λ_1, B for λ_2, and C for λ_3) is associated with one laser amplifier. I, q, and V are the injection current, elementary charge, and cavity volume, respectively, and they are equal for all lasers. The injected carriers are recombined through the stimulated emission to different cavity modes and through the other interband transitions. The rate of stimulated emission is given by the second term on the right-hand side of (1), where v is the speed of light in the medium, and $\xi = \sqrt{\varepsilon\mu^{-1}}/(2\hbar\omega v)$ is the conversion factor that transforms the square of the absolute value of the electric field to photon density. The factor 2 in front of ξ in (1) results from the presense of the two counterpropagating electric fields.

The diagonal matrix $\mathbf{G}_j(\mathbf{n})$ contains the modal gains of each laser for mode j. The absolute value in (1) is applied to each component of $\mathbf{E}_j$ independently. Other interband transitions (mainly nonradiative interband transitions and spontaneous emission) are described by the simple term $\mathbf{n}/\tau$, where τ is the average lifetime of the carriers close to the lasing threshold.

The rate equations for the electric fields $\mathbf{E}_j$ are divided in three terms. The first term in the brackets in (2) is diagonal and describes the interaction of the field with the carriers. The diagonal matrices $\boldsymbol{\alpha}_j$ and $\Delta\boldsymbol{\omega}_j(\mathbf{n})$ contain the cavity losses of the mode j and the displacements of the frequency of the mode j from the corresponding cavity resonance, respectively. Length of the cavity is denoted by L and $\mathbf{E}_j^{\text{ext}}$ is a vector describing the fields injected from outside the cavity. The coupling matrix $\mathbf{M}_j$ in the last term is off-diagonal and describes the coupling between the lasers. The diagonal elements of the gain matrix $\mathbf{G}_j(\mathbf{n})$ are given by

$$[\mathbf{G}_j(\mathbf{n})]_{m,m} = \frac{G_{\max}(\mathbf{n}_m - n_{\text{nom}})}{(\mathbf{n}_m + n_{\text{nom}})(1 + 2\xi\epsilon|(\mathbf{E}_j)_m|^2)} \tag{3}$$

where $G_{\max}$ is the maximum modal gain of the laser, n_{nom} is the carrier density required to achieve transparency, and ϵ is the gain compression factor (accounting only for spectral effects). The diagonal elements of $\Delta\boldsymbol{\omega}_j(\mathbf{n})$ are obtained from

$$[\Delta\boldsymbol{\omega}_j(\mathbf{n})]_{m,m} = \alpha_{\text{lef}}[\Delta\mathbf{G}_j(\mathbf{n})]_{m,m} \tag{4}$$

where α_{lef} is the linewidth-enhancement factor (LEF) and $[\Delta\mathbf{G}_j(\mathbf{n})]_{m,m} = [\mathbf{G}_j(\mathbf{n})]_{m,m} - G_{\text{lef}}$ is the change in the gain with respect to the reference gain at which $(\Delta\boldsymbol{\omega}_j)_{m,m}$ is zero for the signal frequency. The reference gain in this work is set to $G_{\text{lef}} = \alpha_L$, where α_L is the loss for the laser mode.

B. Interactions Between the Components

To model the two structures represented in Fig. 1, the matrices and vectors that adequately describe the properties of individual components and their interactions with each other are needed. The schematic structure shown in Fig. 1(a) is described by (1) and (2), when

$$\mathbf{M}_U = \sqrt{T_L T_s}\begin{bmatrix} 0 & t_a \\ 0 & 0 \end{bmatrix} \tag{5}$$

$$\mathbf{M}_B = \sqrt{T_L T_s}\begin{bmatrix} 0 & 0 \\ t_a & 0 \end{bmatrix} \tag{6}$$

$$\mathbf{M}_C = \mathbf{0} \tag{7}$$

$$\mathbf{E}_U^{\text{ext}} = \sqrt{T_s}[t_b \quad 0]^{\text{T}} E_{L,\max}^{\text{out}} \tag{8}$$

$$\mathbf{E}_B^{\text{ext}} = \sqrt{T_s}[0 \quad t_b]^{\text{T}} E_{L,\max}^{\text{out}} \tag{9}$$

$$\mathbf{E}_C^{\text{ext}} = \sqrt{T_s}[s_U(t) \quad s_B(t)]^{\text{T}} \tag{10}$$

$$\boldsymbol{\alpha}_U = \begin{bmatrix} \alpha_L & 0 \\ 0 & \alpha_s \end{bmatrix} \tag{11}$$

$$\boldsymbol{\alpha}_B = \begin{bmatrix} \alpha_s & 0 \\ 0 & \alpha_L \end{bmatrix}. \tag{12}$$

The elements of the matrices are associated with the lasers L_1 and L_2 of Fig. 1(a), in the given order. The effective transmission coefficients of the laser facets for the optical power at laser mode and the signal mode frequencies are given by T_L and T_s, respectively. Using the square roots of T_L and T_s to obtain the transmission coefficients for the electric field neglects the possible changes in the permittivity of the waveguide and the phase shifts associated with transmission. This can be done without loss of generality in this case. Coefficients t_a and t_b are the transmission coefficients of the appropriate waveguides for the electric field, $E_{L,\max}^{\text{out}}$ is the electric field corresponding to the maximum output power of the lasers and $s_U(t)$ and $s_B(t)$ are external signals that are injected into the control mode (λ_3) of the lasers. The loss of the laser mode is denoted by α_L. The loss for the signal modes α_s is larger than α_L to disable lasing in these cavity modes.

To model the more complicated structure shown in Fig. 1(b), the following coupling matrices are used:

$$\mathbf{M}_U = \begin{bmatrix} 0 & C & iC & iB & B & 0 \\ C & 0 & 0 & iA & A & 0 \\ iC & 0 & 0 & 0 & 0 & 0 \\ iB & iA & 0 & 0 & 0 & 0 \\ B & A & 0 & 0 & 0 & 0 \\ 0 & 0 & 0 & 0 & 0 & 0 \end{bmatrix} \tag{13}$$

$$(\mathbf{M}_B)_{n,m} = (\mathbf{M}_U)_{7-n,7-m} \tag{14}$$

$$\mathbf{M}_C = \mathbf{0} \tag{15}$$

$$A = \frac{1}{4}\sqrt{T_L T_s} g_A t_A^2 \tag{16}$$

$$B = \frac{1}{4\sqrt{2}}\sqrt{T_L T_s} g_A t_A t_B \tag{17}$$

$$C = \frac{1}{2} T_L t_C. \tag{18}$$

The terms t_A, t_B, and t_C are the waveguide transmission coefficients for the electric field and g_A is the amplification of the electric field in the optional amplifier compensating for the losses of the waveguide junctions. The vectors describing the external injection are zero, except for $\mathbf{E}_C^{\text{ext}} = [0 \;\; s_U(t) \;\; is_U(t) \;\; is_B(t) \;\; s_B(t) \;\; 0]^{\mathrm{T}}$. The loss matrix $\boldsymbol{\alpha}_j$ of each laser is diagonal and given by $\boldsymbol{\alpha}_U = \text{Diag}[\alpha_L \;\; \alpha_L \;\; \alpha_L \;\; \alpha_s \;\; \alpha_s \;\; \alpha_s]$, $\boldsymbol{\alpha}_B = \text{Diag}[\alpha_s \;\; \alpha_s \;\; \alpha_s \;\; \alpha_L \;\; \alpha_L \;\; \alpha_L]$, and $\boldsymbol{\alpha}_C = \text{Diag}[\alpha_s \;\; \alpha_s \;\; \alpha_s \;\; \alpha_s \;\; \alpha_s \;\; \alpha_s]$, where the operator Diag constructs a diagonal matrix from the vector following it. The elements of the matrices and vectors are associated to the lasers $\mathrm{L}_{B1}, \mathrm{L}_1, \mathrm{L}_{A1}, \mathrm{L}_{A2}, \mathrm{L}_2$, and L_{B2} of Fig. 1(b), respectively.

C. Simplified Steady-State Model and Stable Points

A detailed discussion on solving (1) and (2) analytically for the steady state of the simplified ideal case [Fig. 1(a) and coupling matrices of (5)–(12)] is given in the appendix. Here some of the most important results are presented in a compact form.

The feedback equation of the simple steady-state model can be presented in the form

$$E'_U = \sqrt{1 - |t'_a\sqrt{1 - |t'_a E'_U + t'_b|^2} + t'_b|^2} \tag{19}$$

where E'_U, t'_a, and t'_b describe the laser mode of L_1 and the waveguide transmission coefficients of the waveguide network [Fig. 1(a)] scaled according to

$$(\mathbf{E}_U)_1 = E'_U E^{\text{out}}_{L,\max}/\sqrt{T_L} \tag{20}$$

$$t_a = (\alpha_s - G_s)L/\sqrt{T_s T_L G_s/G_L}\, t'_a \tag{21}$$

$$t_b = (\alpha_s - G_s)L/\sqrt{T_s T_L G_s/G_L}\, t'_b = \frac{t_a t'_b}{t'_a}. \tag{22}$$

Stable points of the system are located at the points where the feedback equation (19) is fulfilled. This condition is demonstrated graphically in Fig. 2.

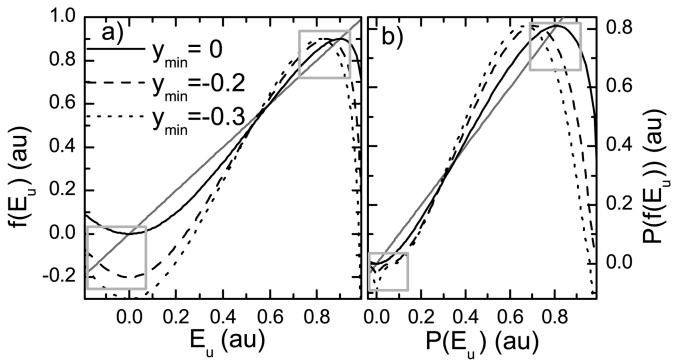

Fig. 2. (a) Left- and right-hand sides of the analytic feedback equation of the COFF [(19)] for three values of $y_{\min}$. Function f denotes either side of the feedback equation. (b) Corresponding values in the power domain for easier comparison with the results presented later. Function P transforms the electric field into optical power. The gray curves correspond to the left-hand side of (19). The stable points are found inside the boxes at the crossings of the gray line with the other curves (the crossings in the middle are labile). In the power domain, negative values are assigned to signals that have negative electric field in (a). Parameter $y_{\max}$ is 0.9 for all plots.

The values of t'_a and t'_b characterize the stable states and the steady-state operation of the flip-flop and they are obtained from

$$t'_b = \frac{-y_{\min} + y_{\max}\sqrt{1 - y^2_{\max}}}{\sqrt{1 - y^2_{\max}} - 1} \tag{23}$$

$$t'_a = y_{\max} - t'_b \tag{24}$$

where parameters $y_{\min}$ and $y_{\max}$ are the minimum and maximum values of the scaled electric field of the feedback signal (value 1 is equivalent to the value of feedback which is required to saturate the laser amplifier). Substituting $y_{\max} = 0.9$ to leave always at least 19% of the maximum power in the laser mode to prevent saturation, and $y_{\min} = -0.3$ results in $t'_a = 2.1$ and $t'_b = -1.2$, the values used in this work. Fig. 2 shows a plot of both sides of (19) for three different values of $y_{\min}$.

Note that for passive waveguides ($t_a < 1, t_b < 1$), (21) and (22) give a maximum for the term $(\alpha_s - G_s)L/\sqrt{T_s T_L G_s/G_L}$ after fixing t'_a and t'_b. Especially the upper limit obtained for the expression $\alpha_s - G_s$ is important, because it directly affects the operating speed of the flip-flop. For the coupling matrices of the more complicated model [(13) and (14)] similar conditions for the waveguides to be passive become

$$t_A^2 = 4\frac{(\alpha_s - G_s)L\sqrt{G_L}}{g_A\sqrt{T_s T_L G_s}} t'_a < 1 \tag{25}$$

$$|t_B| = \left|\sqrt{2} t_A \frac{t'_b}{t'_a}\right| < 1. \tag{26}$$

In other words, when passive waveguides (i.e., $t_A, t_B \leq 1$) are used in the more complete configuration, the maximum value of $\alpha_s - G_s$ in (25) can be controlled by the value of the additional amplification g_A, in addition to the other laser parameters. Therefore, the maximum achievable operating speed can be easily increased by increasing g_A.

D. Phase Locking

An external master laser can be used to provide a reference phase for a slave laser to lock onto. If the frequency of the master laser is not at resonance with a cavity mode of the slave laser, there will be a constant phase difference between the phase of the master and the slave. This phase difference is easily found from (2) when it is written for a single laser and when the time derivative is set to zero

$$E_U = \frac{(G_U - \alpha_U - i\Delta\omega)E_U^{\text{ext}}}{L|G_U - \alpha_U + i\Delta\omega|^2}. \tag{27}$$

The additional phase shift can still be simplified by linearizing the gain and the change in the resonance frequency. The linearized gain is $G_U = \alpha_U + G'_U\Delta n$, where G'_U is the differential gain for the laser mode, $\Delta n = n - n_0$ is the change in the carrier density with respect to the threshold carrier density n_0, determined by the relation $G_U(n_0) = \alpha_U$. The linearized change in resonance frequency is correspondingly $\Delta\omega = \alpha_{\text{lef}}G'_U\Delta n'$, where $\Delta n' = n - n'_0$ is the change in the carrier density, now with respect to n'_0, the carrier density at which the cavity is resonant with the master laser frequency. With the linearizations the term determining the phase shift becomes $G_U - \alpha - i\Delta\omega \approx G'_U n\,(1 - i\alpha_{\text{lef}}\Delta n'/\Delta n)$. As n_0 and n'_0 in this work are equal, the phase shift becomes simply equal to the phase of the constant $1 - i\alpha_{\text{lef}}$.

The phase shift of the phase locking for a given LEF value in equilibrium is constant. Therefore, it is fairly easy to compensate for it by adjusting the phase shifts of the waveguides connecting the lasers.

IV. Numerical Simulations and Discussion

Understanding the operation characteristics of any memory element culminates in understanding why, how and under what circumstances the device changes its state. In this section, these questions are investigated numerically by solving the rate equations for some transient processes in the system described by the matrices of Section III-B and by the parameter values of Table I. Most of the parameter values shown in Table I are typical of semiconductor lasers. However, there are a few parameters (most notably $G_{\max}, n_{\text{nom}}, \alpha_{\text{lef}}$, and L), for which the given values are better than typical. These parameter values correspond to optimum performance within the limits of technological feasibility. Results calculated for less favorable parameter values are also discussed later.

The current configuration is unideal in the sense that there are no actual optical isolators and that the master lasers are also included in the model. In contrast it is ideal in the sense that the phase shifts and transmission coefficients of the antireflectors are set to the values needed for perfect destructive interference.

A. Basic Operation

To compare the stable states of the system with the results of Section III-C, the feedback from laser L_2 to laser L_1 is temporarily replaced by an independent signal at λ_2 sweeping from $E_{\min}$ to $E_{\max}$ in 2 ns. Fig. 3 shows the results of the sweep. Instead of changing $y_{\min}$, like in Section III-C, it is kept at $y_{\min} = -0.3$, and the curves are plotted for three different values of LEF. The outcome is reasonably similar to the result found in Section III-C for the ideal analytical model, especially when taking into account that Fig. 3 is extracted from transient data and that in Section III-C it was possible to encode the phase of the signal into the presented values of power (i.e., the negative values of power represented the phase shift of 180°). The effect of LEF is seen to be small.

In order to demonstrate how the COFF changes state, short pulses are send to the SET and RESET ports. Fig. 4 shows the pulses at the SET and RESET ports (dark and light gray curves, respectively) and the output of the COFF for the same three values of LEF as in the previous figure. The SET and RESET pulses are repeated at a frequency of 1.6 GHz, with length of

TABLE I
Parameter Values Used in the Calculations

Symbol	Value	Comment
I	4.2 mA	Injection current
V	9 μm^3	Volume of the optical cavity
L	10 μm	Length of the cavity
n_r	3	Refractive index
τ	1 ns	Carrier lifetime excluding stim. emission
$\hbar\omega$	1 eV	Photon energy
$G_{\max}$	10^5/m	Maximum gain
n_{nom}	10^{22} m^{-3}	Transparency carrier density
ϵ	10^{-23} m^3	Gain compression factor
α_L	10536/m	Loss coefficient for the lasing mode
α_s	16687/m	Loss coefficient for the other modes
T_L	0.1	Reflectivity for power at laser mode
T_s	0.154	Reflectivity for power at signal mode
ξ	$\frac{1}{2\hbar\omega v}\sqrt{\varepsilon/\mu}$	$\xi\lvert\text{E-field}\rvert^2 \rightarrow$ photon density
α_{lef}	0-1	Linewidth enhancement factor
t_A	ϕ_0	Waveguide transmission (E-field)
t_B	-0.808ϕ_0	Waveguide transmission (E-field)
t_C	$2\times10^{-2}\phi_0$	Waveguide transmission (E-field)
g_A	4	Gain (E-field)
ϕ_0	$\frac{1+i\alpha_{lef}}{\lvert1+i\alpha_{lef}\rvert}$	Waveguide phaseshift

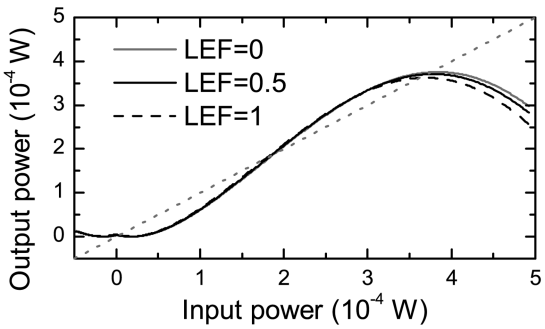

Fig. 3. Numerically calculated output of the COFF as a function of an input signal applied to the SET port when no feedback from L_2 to L_1 is present (compare with Fig. 2). The output power is smaller than the nominal 2-mW output power of a single laser amplifier because it is partly canceled by the interference with the bias signal.

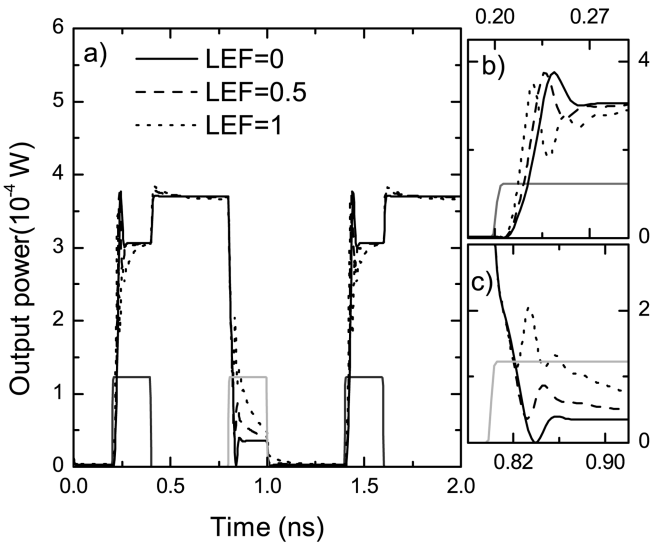

Fig. 4. (a) Power at the output port while SET (dark gray) and RESET (light gray) pulses are applied to the input. The smaller figures show a magnification of (a) at the moment of applying (b) the first SET or (c) the RESET pulse. The SET pulse makes the output high until a RESET pulse is applied, and vice versa.

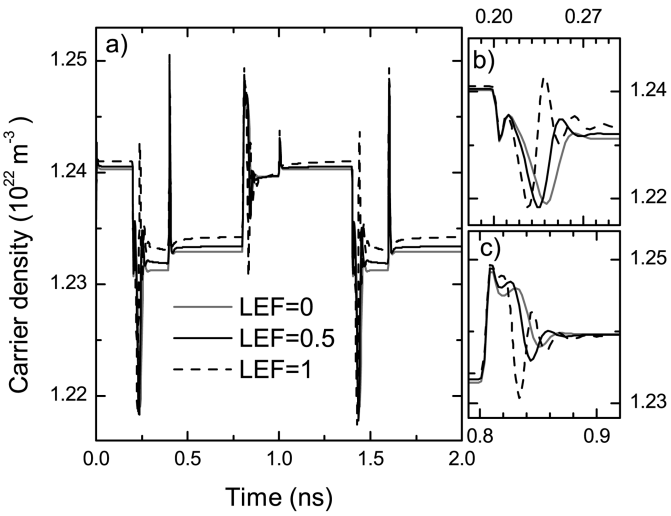

Fig. 5. (a) Carrier density in L_1 when the SET and RESET pulses of Fig. 4 are applied at the input. When the input signal changes, the photon - carrier interaction causes the carrier density to compensate for the growing or decreasing photon density in the laser cavity. The smaller figures show a magnification of (a) at the moment of applying (b) the SET or (c) the RESET pulse. Note that the change in the carrier density between the steady states is only $\sim 0.5\%$ and the maximum change from average value is 1.2% for transients.

0.2 ns (5 GHz). Unlike in the unbiased flip-flop (not shown), the output starts to change almost instantly after the SET or RESET pulse is applied to the input.

Fig. 4 demonstrates a number of other interesting properties as well. First, it gives the timescale the system needs to reach equilibrium. This is found to be about 80 ps or 12 GHz. Time to actually switch states is shorter than this and reaching equilibrium is not necessary before changing states is possible again. Faster switching speeds are studied later. Second, the LEF is clearly seen to affect the time needed to reach equilibrium, even if the static behavior for different values of LEF is almost identical. [The relaxation of the system to the new state is seen better in the phase plot, presented later in Fig. 6(b).]

A significant property is also the absence of relaxation oscillations for low LEF, when the product of the photon density and the differential gain is sufficiently high [13]. In Fig. 4, this property is seen for $\mathrm{LEF} = 0$ (the solid line). The single peak in the curve at the moment of applying the SET pulse is not a result of relaxation oscillations, but is caused by the dynamics of the feedback signal, which passes by zero when the state changes. When the feedback is zero, the output peaks and then sets to a lower value when the feedback reaches its nonzero steady-state value.

Figs. 5 and 6 show the carrier density, the phase of the electric field of the laser mode, and the power in the lasing mode in L_1 during the operation. When the input signal changes, the system is driven out of equilibrium, and the carrier–photon interaction causes changes in the carrier density in order to compensate for the change in the total optical power in the cavity. In the steady state, the carrier density then sets to a static value, which is almost the same for the two states (note the scale in Fig. 5). The same phenomena are also observed in the total optical power of the laser and the phase of the laser mode. The carrier density and optical power recover reasonably fast from the perturbation when LEF is small. For larger values of LEF the recovery takes

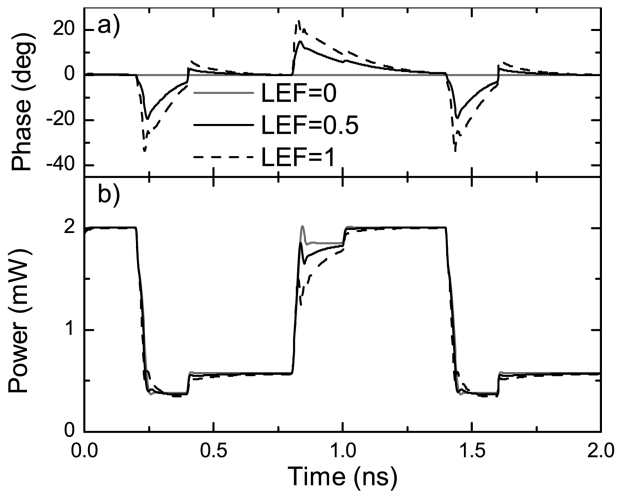

Fig. 6. (a) Phase of the laser mode of L_1 relative to the phase of the master laser for the SET and RESET pulses shown in Fig. 4. The changes in the carrier density result in changes in the optical length of the cavity which, in turn, alters the phase shift that the phase-locking signal undergoes in the cavity. The device can, however, be adjusted in such a way that in the steady state, the phase shift is roughly constant. (b) Corresponding output power of the laser mode. The changes in the input signal affect the optical power of the laser mode through the changes in the carrier density and gain. The power of the laser does not reduce to zero in either state.

longer. The speed of the phase relaxation could be increased by making the coupling strength of the phase locking stronger.

B. Other Operational Characteristics

Apart from the use as a memory element, the basic consept of COFF can also be used to realize other logic functions. A similar construction without feedback has already been proposed as a way to realize a reamplifying, reshaping (2R) regenerator and other arbitrary functions [13]. Adding feedback to the structure

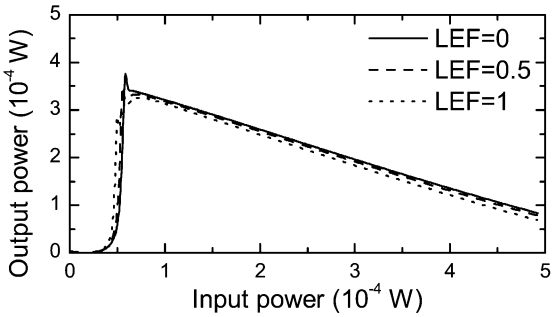

Fig. 7. Response of the COFF to an input signal in the SET port. There is a clear threshold in the SET-operation.

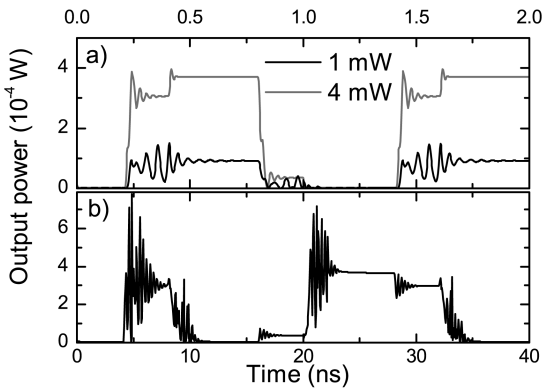

Fig. 8. (a) Relaxation oscillations are clearly seen when the total output power (i.e., the injection current) or the differential gain of the lasers is decreased. Here the transparency carrier density is increased to $10^{23}\mathrm{m}^{-3}$, $\alpha_{\mathrm{lef}} = 0$ and values 1 and 4 mW are used for the total output power. (b) If the device parameters are made even less favorable ($G_{\max} = 10\,000/\mathrm{m}$, $n_{\mathrm{nom}} = 10^{23}\mathrm{m}^{-3}$, $L = 100\ \mu\mathrm{m}$, $\alpha_{\mathrm{lef}} = 1$), the relaxation oscillations get stronger and the operation slows down. For higher values of LEF, the device may become unstable and start to oscillate.

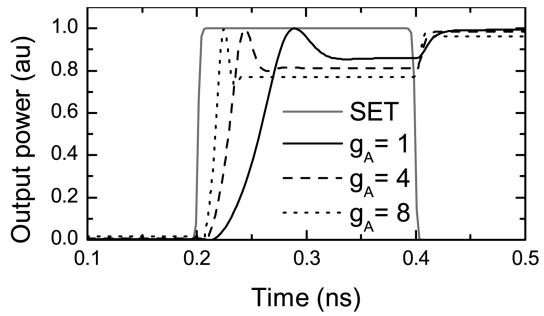

Fig. 9. Rise time of the device decreases approximately inversely proportional to the term $\alpha_s - G_s$. The term α_s can be increased for example by increasing the value of the additional amplification g_A in the feedback path. A value $g_A = 8$ allows a rise time of <14 ps, which corresponds roughly to 71 GHz. LEF is set equal to zero in this calculation.

makes the construction more versatile, but also difficult to model analytically. Fig. 7 shows the strong nonlinearity of the COFF, caused by the feedback. An optical signal with increasing power is applied to the SET-port. At the switching threshold, the output (at λ_2) is seen to grow steeply. The LEF has only minor effect on the location of the threshold. The strong nonlinearity also suggests good regenerative properties for a similar construction, where feedback is altered so that there is only one stable state when there is no input.

The small signal analysis of a single laser amplifier predicts the disappearance of relaxation oscillations for high optical power–differential gain product [13]. Because of the presence of feedback, it is not possible to apply this result directly to the COFF structure. Nor is it possible to make a similar analytical study. However, the numerical simulations in Figs. 4 and 8 indicate that there is a threshold for the disappearance of relaxation oscillations. In Fig. 4 for $\alpha_{\mathrm{lef}} = 0$ no relaxation oscillations are visible. For nonzero values of LEF there are small relaxation oscillations, such as fluctuations in the lasers which are absent when $\alpha_{\mathrm{lef}} = 0$. The mechanism producing this effect is likely to involve several lasers and the coupling between them rather than only the carrier density and optical fields of a single laser. In Fig. 8, clearly visible conventional relaxation oscillations are then found for low optical power–differential gain product. Also the slowing down of the COFF with high transparency carrier density, low modal gain and longer cavity is shown in Fig. 8(a).

The approximately linear dependence of the maximum operating speed on the term $\alpha_s - G_s$, also found by small signal analysis of a single laser amplifier [13], is qualitatively verified as well: the rise time of the signal decreases as $\alpha_s - G_s$ increases (see Fig. 9). This can be achieved for example by increasing the additional amplification g_A in the feedback path. Increasing g_A from 1 to 8 decreases the rise time approximately from 0.061 ns (16 GHz) to 0.014 ns (71 GHz), i.e., by a factor of 4.4. There should be no fundamental reason why the speed could not be increased even further. This implies that very high operating speeds could be achieved, especially with the new manufacturing methods and active materials, like quantum dots.

The most significant error sources in the present model are the absence of any noise sources, neglecting the propagation delays between the lasers, the rate-equation model itself, and some idealizations made in parametrizing the structure. The first three of these effects are not considered to be overly important: the noise in coherent laser beams is known to be small, the propagation delay between the cavities is relatively small, and the rate equations have proven to be an adequate model for lasers. However, making the waveguide junctions forming the antireflectors less ideal (i.e., making the two arms of the interferometer or the lasers L_{A1} and L_{A2} slightly asymmetric) potentially reduces the stability, if the strength of the phase locking is not increased correspondingly.

V. Conclusion

This work describes a new method of providing the nonlinear feedback needed to construct optical flip-flops by using coherent optical bias fields on the feedback paths of the device. The method does not require operating the laser amplifiers below the lasing threshold. Therefore, there is always a large photon population present in the laser mode. This allows a far better response to incoming signals than in the conventional all-optical flip-flops where the nonlinearity is provided by the abrupt change in the output power taking place at the lasing threshold.

The behavior of the flip-flop is modeled by a set of rate equations describing the carrier densities and complex electric fields

in each laser. Although the rate equation models are well known and reasonably accurate, the results should be interpreted as a demonstration of concept rather than an in depth study of all the properties of the flip-flop. Still, the results do show promise of a fast integrated optical memory for specific small scale applications. With small modifications the originally modest nonlinearity enhanced by feedback could also be used to realize logical operations. Furthermore, despite the complexity of the structure, processing prototypes should be possible even with today's technology.

APPENDIX

In this appendix, the results presented in Section III-C for the steady state of the simplified ideal case [Fig. 1(a) and coupling matrices of (5)–(12)] are derived from (1)–(2). In steady state, the time derivatives of (1)–(2) are zero. Also, the rate equation of the control signal [C in (2)] is removed, the control signal itself ($\mathbf{E}_C$) is set to zero and the phase fluctuations are neglected ($\Delta\boldsymbol{\omega} = \mathbf{0}$). These simplifications give a new set of equations

$$0 = \frac{I}{qV} - 2\xi v\left(G_L\left|E_L^m\right|^2 + G_s\left|E_s^m\right|^2\right) - \frac{n_m}{\tau} \quad (28)$$

$$0 = \frac{v}{2}(G_L - \alpha_L)E_L^m + \frac{v}{2L}E_L^{m,\mathrm{ext}} \quad (29)$$

$$0 = \frac{v}{2}(G_s - \alpha_s)E_s^m + \frac{v}{2L}\sqrt{T_s}\left(\sqrt{T_L}t_a E_L^{3-m} + t_b E_{L,\max}^{\mathrm{out}}\right) \quad (30)$$

where the notation is changed so that vectors are replaced by scalars, $m \in \{1,2\}$ indexes the laser (L_1 or L_2), E_L^m denotes the laser mode and E_s^m the feedback mode of laser m. Approximating that the phase locking terms $E_L^{m,\mathrm{ext}}$ are effectively zero, (29) states that, while above the laser threshold, the gain of the structure is $G_L(n_m) = \alpha_L$. Therefore, the carrier density only depends on the losses, which are constant. From (28) it follows that

$$G_L|E_L^m|^2 + G_s\left|\frac{\sqrt{T_s}\left(\sqrt{T_L}t_a E_L^{3-m} + t_b E_{L,\max}^{\mathrm{out}}\right)}{(\alpha_s - G_s)L}\right|^2 = \left(\frac{I}{qV} - \frac{n_m}{\tau}\right)/(2\xi v) = G_L\left|E_{L,\max}^{\mathrm{out}}\right|^2/T_L \quad (31)$$

is constant [after substituting E_s^m solved from (30)]. Rescaling (31) with (20)–(22) results in rescaled formulas (note that in Section III-C, notation E_U' is used for $E_L^{1\prime}$ and $E_L^{2\prime}$ is scaled according to the same formula as $E_L^{1\prime}$)

$$E_L^{1\prime} = \sqrt{1 - \left|t_a' E_L^{2\prime} + t_b'\right|^2} \quad (32)$$

$$E_L^{2\prime} = \sqrt{1 - \left|t_a' E_L^{1\prime} + t_b'\right|^2}. \quad (33)$$

Eliminating $E_L^{2\prime}$ from these gives the feedback equation (19).

To determine the possible range of values for the parameters t_a' and t_b', a transformation of variables is made with $y_1 = t_a' E_L^{2\prime} + t_b'$ and $y_2 = t_a' E_L^{1\prime} + t_b'$. This results in

$$y_1 = t_a'\sqrt{1 - |y_2|^2} + t_b' \quad (34)$$

$$y_2 = t_a'\sqrt{1 - |y_1|^2} + t_b' \quad (35)$$

where y_m now represent the electric field of the feedback signals injected to the feedback mode of the lasers. Because of the symmetry of the structure, fields y_1 and y_2 must have the same range of possible values, i.e., $y_1, y_2 \in [y_{\min}, y_{\max}]$. Concentrating on the most interesting segment of solutions where $y_{\min} \le 0, y_{\max} > -y_{\min}$ and $t_a' > 0$, an equation relating the parameters $t_a', t_b', y_{\min}$, and $y_{\max}$ can be written as

$$y_{\max} = t_a' + t_b' \quad (36)$$

$$y_{\min} = t_a'\sqrt{1 - y_{\max}^2} + t_b'. \quad (37)$$

Solving for t_a' and t_b' then gives (23)–(24).

REFERENCES

[1] K. Otsuka, "All-optical flip-flop operations in a coupled element bistable device," *Electron., lett.*, vol. 24, pp. 800–801, June 1988.

[2] M. T. Hill, H. de Waardt, G. Khoe, and H. Darren, "All-optical flip-flop based on coupled laser diodes," *IEEE J. Quantum Electron.*, vol. 37, no. 3, pp. 405–413, Mar. 2001.

[3] H. Kawaguchi, I. H. White, M. Offside, and J. E. Carroll, "Ultrafast switching in polarization-bistable laser diodes," *Opt. Lett.*, vol. 17, pp. 130–132, Jan. 1992.

[4] F. Robert, D. Fortusini, and C. Tang, "All-optical set-reset operation of a bistable semiconductor laser intracavity-coupled to a vertical cavity surface-emitting laser," *IEEE Photon. Technol. Lett.*, vol. 12, no. 5, pp. 465–467, May 2000.

[5] G.-H. Duan, P. Landais, and J. Jacquet, "Modeling and measurement of bistable semiconductor lasers," *IEEE J. Quantum Electron.*, vol. 30, no. 11, pp. 2507–2515, Nov. 1994.

[6] P. Blixt and U. Ohlander, "19 ps switching of a bistable laser diode with 30 fJ optical pulses," *IEEE Photon. Technol. Lett.*, vol. 2, no. 3, pp. 175–177, Mar. 1990.

[7] M. Takenaka and Y. Nakano, "Multimode interference bistable laser diode," *IEEE Photon. Technol. Lett.*, vol. 15, no. 8, pp. 1035–1037, Aug. 2003.

[8] Y. Liu, M. Hill, H. de Waardt, G. Khoe, D. Lenstra, and H. Dorren, "All-optical flip-flop memory based on two coupled polarization switches," *Electron. lett.*, vol. 38, pp. 904–906, Aug. 2002.

[9] M. T. Hill, H. J. S. Don-en, T. de Vries, X. J. M. Leijtens, J. H. den Besten, B. Smalbrugge, Y.-S. Oei, H. Binsma, G.-D. Khoe, and M. K. Smit, "A fast low-power optical memory based on coupled micro-ring lasers," *Nature*, vol. 432, pp. 206–209, Nov. 2004.

[10] M. T. Hill, H. de Waardt, G. D. Khoe, and H. J. S. Dorren, "Fast optical flip-flop by use of mach zehnder interferometers," *Microw. Opt. Technol. Lett.*, vol. 31, pp. 411–415, Dec. 2001.

[11] R. Paiella, R. Martini, F. Capasso, C. Gmachl, H. Y. Hwang, D. L. Sivco, J. N. Baillargeon, A. Y. Cho, E. A. Whittaker, and H. C. Liu, "High-frequency modulation without the relaxation oscillation resonance in quantum cascade lasers," *Appl. Phys. Lett.*, vol. 79, pp. 2526–2528, Oct. 2001.

[12] R. Lang, "Injection locking properties of a semiconductor laser," *IEEE J. Quantum Electron.*, vol. 18, no. 6, pp. 976–983, Jun. 1982.

[13] J. Oksanen and J. Tulkki, "Fast 2R regeneration by coherent laser amplifiers," *IEEE J. Quantum Electron.*, vol. 41, no. 8, pp. 1075–1082, Aug. 2005.

Jani Oksanen was born in Finland in 1977. He received the M.Sc. degree in electrical engineering from Helsinki University of Technology, Espoo, Finland, in 2001, where he is currently pursuing the Ph.D. degree in the Laboratory of Computational Engineering.

Jukka Tulkki received the Ph.D. degree in physics from the Helsinki University of Technology (HUT), Espoo, Finland, in 1986. His thesis addressed inelastic resonance scattering of X-rays.

Since 1998, he has been a Professor of computational engineering at HUT. He is the author or co-author of more than 60 journal papers and numerous conference presentations. His current research interests include X-ray physics, atomic collision physics, semiconductors, electronic and optical properties of mesoscopic systems, and microsystems.